

Cite this: *RSC Sustainability*, 2023, 1, 987

Highly crosslinked polyesters prepared by ring-opening copolymerization of epoxidized baru nut and macaw palm oils with cyclic anhydrides†

Aaron L. Vermiglio,^a Rafael T. Alarcon,^b Éder T. G. Cavalheiro,^b Gilbert Bannach,^c Thomas J. Farmer^b and Michael North^{*a}

Epoxidised Brazilian vegetable oils obtained from the baru nut (*Dipteryx alata* Vogel) and the macaw palm (*Acrocomia aculeata*) react with bioderivable anhydrides (succinic, glutaric, itaconic or citraconic) to give highly crosslinked polyesters. The polymerisation is initiated by a metal-free catalyst system comprising dicyclohexyl urea and bis(triphenylphosphine)iminium chloride. The resulting polymers can be obtained as powders or rubbery disks and are chemically and physically characterised. On treatment with aqueous sodium hydroxide, the polymers degrade to water soluble glycerol and sodium carboxylates.

Received 11th March 2023
Accepted 11th May 2023

DOI: 10.1039/d3su00088e

rsc.li/rscsus

Sustainability spotlight

The work in this paper aligns primarily with UNSDG 12: sustainable consumption and production as it is concerned with the synthesis of highly crosslinked polyesters from epoxides obtained by epoxidation of triglycerides obtained from Brazilian biomass and bioderivable anhydrides. The resulting polymers are shown to be degradable at end of life. Hence, the polymers address sustainability issues at both start and end of life. The overview of UNSDG 12 notes that unsustainable patterns of consumption and production are root causes of climate change, biodiversity loss and pollution. Our approach to a major class of chemicals (polymers) will help to address this.

Introduction

Polymers are ubiquitous in modern life and have been produced commercially for over 100 years. Their global production currently exceeds 360 million metric tonnes per annum.¹ However, both the production and end of life disposal of polymers give rise to serious sustainability issues. Commercial polymers are almost entirely derived from petrochemicals by processes which consume 8% of global oil and gas production, making them second only to transport fuel in the use of oil and gas. Currently, less than 1% of commercial polymers are sustainably sourced.¹ The end of life treatment of polymers is equally problematic with just 9% being recycled. The remainder is either incinerated (12%) resulting in carbon dioxide emissions or discarded on land or in the oceans² (79%) causing major pollution problems.³ Thus a major challenge in green chemistry is the development of new polymers which are sustainably sourced and degradable at end of life. This will allow

the development of a sustainable and potentially circular economy for polymers,⁴ but requires the integrated consideration of feedstocks, production methodology and design for degradation.

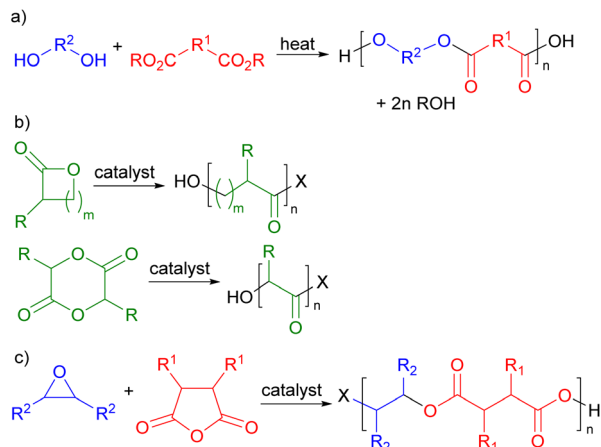
Polyesters have great potential to address these sustainability issues. They are potentially chemically degradable at end of life by hydrolysis of their backbone ester bonds, making them more recyclable than many other classes of widely used polymers.⁵ In addition, the oxygenated functional groups needed to produce monomers for polyester synthesis are commonly found in biomass, giving polyesters the potential to be biosourced. There are three main routes for the production of polyesters. Commercially, the most developed synthesis is the thermally induced condensation polymerization between a diol and a diacid or diester (Scheme 1a)⁶ which, for example, is used in the production of poly(ethylene terephthalate) (PET).⁷ Since many diacids and diols are readily available from biomass, it should be possible to prepare sustainably sourced polymers in this way. However, the harsh thermal conditions⁸ needed to drive this process to high molecular weights (220–260 °C for PET⁹) limit the functional groups that can be present in the monomers. An alternative approach to polyester synthesis involves the ring-opening polymerisation of lactones or lactides (Scheme 1b)¹⁰ which is used in the commercial production of poly(caprolactone) and poly(lactic acid).¹¹ This is a lower temperature, catalysed process which is already being used with

^aGreen Chemistry Centre of Excellence, Department of Chemistry, University of York, York, YO10 5DD, UK. E-mail: michael.north@york.ac.uk; thomas.farmer@york.ac.uk

^bSão Carlos Institute of Chemistry, USP – University of São Paulo, 13566-590, São Carlos, SP, Brazil

^cSchool of Sciences, Department of Chemistry, UNESP – São Paulo State University, 17033-260, Bauru, SP, Brazil

† Electronic supplementary information (ESI) available. See DOI: <https://doi.org/10.1039/d3su00088e>



Scheme 1 Routes for the synthesis of polyesters. (a) Condensation polymerisation. (b) Ring-opening polymerization. (c) Ring-opening copolymerization.

biomass derived monomers, but the range of potential monomers is rather limited. The third approach to polyester synthesis is the ring-opening, alternating copolymerization (ROCOP) of epoxides and cyclic anhydrides (Scheme 1c).¹² ROCOP is a lower temperature catalysed process, so it is also compatible with functionalized monomers. Cyclic anhydrides are readily prepared from diacids and epoxides can be formed by the epoxidation of alkenes; so the ROCOP route to polyesters is also compatible with sustainably sourced monomers.

ROCOP is a living polymerization process that is capable of producing polymers with narrow molecular weight distributions. However, it is also very susceptible to chain-transfer by adventitious moisture which reduces the molecular weight of the polymer. As a result, ROCOP is typically carried out under rigorously inert and anhydrous conditions involving the use of a glove box. Recently, we reported that ROCOP of functionalised biomass derivable anhydrides and epoxides could be carried out with both metal-based and metal-free initiators without the need for a glove box or other specialised equipment.¹³ Although the linear polyesters formed had rather low molecular weights due to moisture induced chain-transfer, the functionality they possessed (alkenes and alkyl halides) allowed them to be crosslinked to produce insoluble, polyester derived resins. This approach worked well, but did require two steps and a non-biobased crosslinking agent. We realised that both these factors could be avoided if instead of using simple mono-epoxides as monomers, a biomass derived monomer containing multiple epoxides was used. This would allow the one-step synthesis of completely sustainably sourced crosslinked polyester resins. In addition, the detrimental effect of chain-transfer would be avoided as each crosslinking polyester chain can be short without compromising the formation of the crosslinked resin.

In previous work we have also reported the synthesis of epoxidised triglycerides obtained from baru nut (*Dipteryx alata Vogel*) and macaw palm (*Acrocomia aculeata*) oils (Fig. 1).¹⁴ Baru nuts and macaw palms are grown commercially in the Cerrado

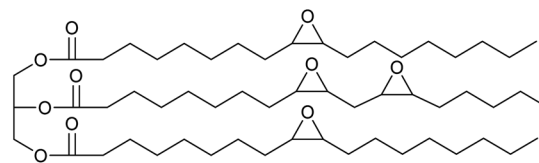


Fig. 1 Simplified structural representations of epoxidised oils **1** and **2**. In reality each fatty acid chain may contain 0–2 epoxides and fewer or more than the 18 carbon atoms shown. On average, **1** contains 3.5 epoxides per triglyceride and **2** contains 4 epoxides per triglyceride.

region of Brazil¹⁵ and produce vegetable oils which are high in polyunsaturated fatty acids. Hence, epoxidation of baru nut oil gave epoxidised baru nut oil **1** containing on average 3.5 epoxides per triglyceride and epoxidation of macaw palm oil gave epoxidised macaw palm oil **2** containing on average 4 epoxides per triglyceride. Therefore, in this paper, we show that ROCOP applied to epoxidised vegetable oils **1** and **2** and biomass derivable anhydrides leads directly to highly crosslinked, insoluble polyester resins. Both the chemical and physical properties of the resins are determined and it is shown that they can be degraded to water soluble sodium carboxylates on treatment with aqueous sodium hydroxide.

Results and discussion

In previous work,¹¹ we showed that both metal-based catalysts (aluminium and chromium salophen complexes) and the organocatalyst dicyclohexyl urea¹⁶ (DCHU, **3**, Fig. 2) were capable of inducing the ROCOP of mono-epoxides and anhydrides in the presence of bis(triphenylphosphine)iminium chloride (PPNCl, **4**) at 100 °C for 15–60 minutes under solvent-free, standard laboratory conditions. Of these catalysts, DCHU is particularly attractive as it is an industrial by-product¹⁷ and will not introduce coloured and/or toxic metal residues into the polymer. Therefore, in this work polymerisations were carried out using the DCHU/PPNCl initiator system. DSC analysis (ESI, Fig. S1†) of a mixture of macaw oil **2**, succinic anhydride **5**, DCHU **3** and PPNCl **4** (250 : 1000 : 1 : 1 ratio) showed that 100 °C was the lowest temperature at which exothermic polymerisation occurred, so this was used as the polymerisation temperature throughout the study (Scheme 2). Reactions were left for 18 hours as initial studies showed that the reaction mixture became highly viscous and then solidified as the crosslinking polymerisation progressed.

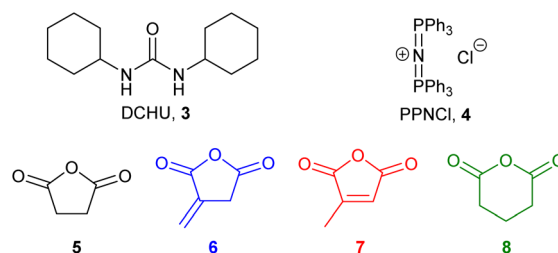
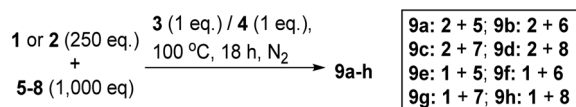


Fig. 2 Structural formulas of initiators **3** and **4** and anhydrides **5**–**8**.





Scheme 2 Synthesis of cross-linked polyesters 9a–h.

Epoxidised macaw palm oil 2 is a liquid at room temperature whilst epoxidised baru nut oil 1 is a low melting point solid. Each of these epoxidised triglycerides were polymerised with four potentially bioderivable anhydrides 5–8. Succinic anhydride 5 can be obtained from succinic acid which is produced commercially by fermentation of sugars.¹⁸ Itaconic anhydride 6 can be produced either from itaconic acid (manufactured by fungal fermentation of sugars¹⁹) or by thermolysis of citric acid.²⁰ Citraconic anhydride 7 is a regioisomer of itaconic anhydride 6. It is a natural product found in coffee and can be manufactured by thermolysis of itaconic or citric acids.¹⁷ Glutaric anhydride can be obtained from the natural product glutaric acid.²¹ Thus a set of eight highly crosslinked polyesters 9a–h was produced as shown in Scheme 2. After polymerisation, the solid polymer mass produce was ground to a powder and subjected to Soxhlet extraction (using dichloromethane, ethyl acetate or ethanol) to constant weight to remove initiators 3 and 4 along with any unreacted monomers, giving polymers 9a–h as white–yellow powders with the percentage yields shown in Table 1. These percentage yields are based on the theoretical incorporation of all of the epoxidised oil (1, 2) and all of anhydrides 5–8. In reality, this cannot be achieved for two reasons. As the polymerisation progresses, the reaction mixture becomes more viscous, so the ROCOP process becomes slower, resulting in unreacted monomers and low molecular weight oligomers being formed which are subsequently removed during the Soxhlet extraction. In addition, ether formation (involving only epoxidised oils 1 or 2) can occur and will result in unreacted anhydride 5–8 being present and subsequently removed during the Soxhlet extraction. Whilst intermolecular reaction of epoxides to form polyethers is only a minor side-reaction in ROCOP using the 3/4 initiator system,¹³ in the case of epoxidised oils 1 and 2, ether formation can occur intramolecularly and this is likely to occur at a rate that is more competitive with ROCOP,

especially as the rate of ROCOP is reduced in the latter stages of the polymerisation.

Thermogravimetric analysis (ESI, Fig. S2–S10†) showed that all of the powdered polymers 9a–h were thermally stable up to *ca.* 250 (9c); 260 (9b, g); 270 (9a, d, f) or 290 °C (9e, h). Polymers derived from baru nut oil (9e–h) all had higher thermal stability and decomposition temperatures (by 12–30 °C) than the corresponding polymer made from the same anhydride and macaw palm oil (9a–d). The polymers derived from unfunctionalised anhydrides 5 and 8 had similar decomposition temperatures (T_{D10}); 340 ± 1 °C for 9a, d and 354 ± 2 °C for 9e, h and these were higher than the corresponding decomposition temperatures of polymers derived from unsaturated anhydrides 6 and 7 ($304\text{--}325$ °C for 9b, c; $334\text{--}339$ °C for 9f, g). The polymers obtained from anhydrides 5 and 8 also presented a higher thermal stability (271 ± 2 °C for 9a, d; 290 ± 5 °C for 9e, h).

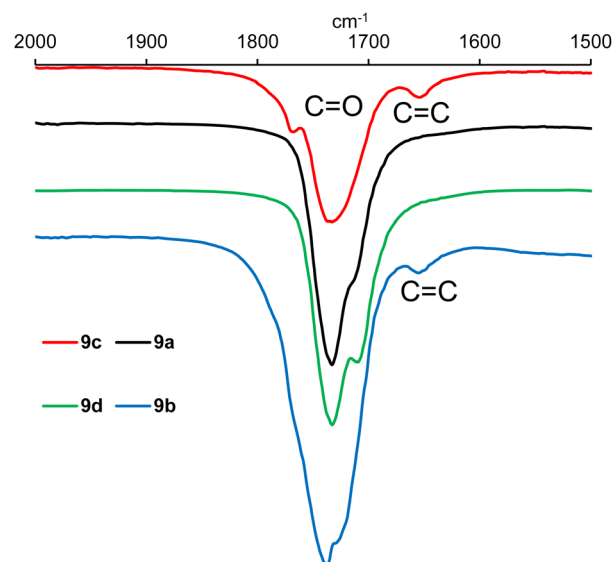
Polymers 9a–h were also analysed by differential scanning calorimetry (DSC) between -60 and 200 °C (ESI, Fig. S11–S18†). Polymers 9a, b, d, h had glass transition temperatures between -5 and -15 °C ($0.3\text{--}0.4$ J g⁻¹), no glass transition temperature was detected for the other four polymers and no other phase changes were detected, suggesting that all of polymers 9a–h were amorphous.

IR analysis of polymers 9a–h (ESI, Fig. S21–S28†) revealed that in the functional group region ($4000\text{--}1600$ cm⁻¹), the spectra were very similar to those of the epoxidised vegetable oil from which they were prepared (ESI, Fig. S19 and S20†), but there were clear differences in the fingerprint region ($1600\text{--}600$ cm⁻¹). However, detailed analysis of the $2000\text{--}1500$ cm⁻¹ region did show the presence of a weak alkene stretching band at 1653 cm⁻¹ in polymers derived from macaw oil and unsaturated anhydrides 6 and 7 as shown in Fig. 3. In the corresponding baru nut oil derived polymers (9e–h), this alkene stretching band was weaker and only clearly visible in polymer 9g derived from anhydride 7 (ESI, Fig. S27†).

Table 1 Yields and thermal properties of powdered polymers 9a–h

Polymer	Yield ^a (%)	T_g^b (°C)	T_{D10}^b (°C)	T_g^b (°C)
9a	67	273	340	-14.9
9b	61	264	325	-5.5
9c	59	253	304	
9d	46	271	341	-14.9
9e	35	295	352	
9f	54	274	339	
9g	59	261	334	
9h	46	290	356	-13.6

^a Percentage yield after Soxhlet extraction and based on the theoretical incorporation of all epoxidised oil and anhydride. ^b Limit of thermal stability temperature (T_g) and temperature at which the polymer has lost 10% of its weight (T_{D10}) determined by thermogravimetric analysis under argon with a heating rate of 10 °C min⁻¹.

Fig. 3 Expansion of the IR spectra of polymers 9a–d between 1500 and 2000 cm⁻¹.

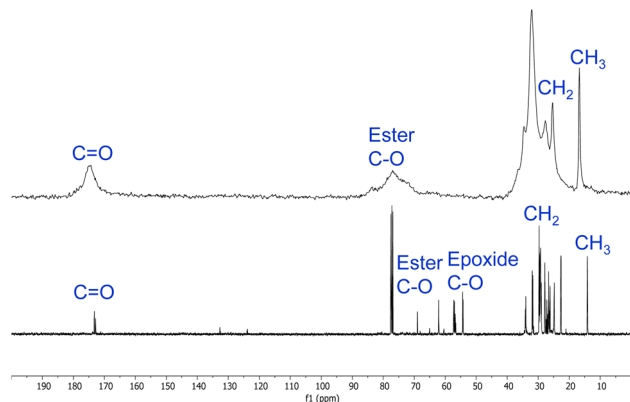


Fig. 4 Comparison of the ^{13}C NMR spectra of epoxidised macaw palm oil 2 (bottom) and polyester **9a** (top).

Polymers **9a–h** were also analysed by solid-state ^{13}C NMR spectroscopy (ESI, Fig. S29–S36[†]). Fig. 4 shows a comparison of the solution state ^{13}C NMR spectrum of epoxidised macaw palm oil 2 and the solid-state ^{13}C NMR spectrum of polymer **9a** derived from 2 and succinic anhydride 5 (the corresponding spectral comparison of epoxidised baru nut oil 1 and polymer **9e** is given in the ESI, Fig. S37[†]). The peaks between 10 and 35 ppm in both spectra correspond to the aliphatic chains of the macaw palm oil and show that the oil has remained intact during the thermal polymerisation. Ester carbonyl peaks are also clearly visible at 170–180 ppm in both spectra. The most significant difference between the two spectra is in the 50–90 ppm range. In the spectrum of epoxidised oil 2, a series of signals corresponding to C–O groups are present. Those in the range 50–60 ppm can be assigned to carbons within epoxide rings, whilst the two signals between 60 and 70 ppm correspond to the esterified glycerol carbons. In the spectrum of polymer **9a**, the epoxide carbons are clearly absent, showing that the polymerisation has gone to completion and a broadened ester C–O signal is present at 70–90 ppm corresponding to both the glycerol esters and the newly formed esters arising from reaction of the epoxides with anhydride 5.

Whilst all eight polymers **9a–h** displayed very similar solid state ^{13}C NMR spectra (ESI, Fig. S29–S36[†]), there were subtle differences between the spectra as illustrated in the 60–200 ppm expansions of polymers **9a–d** shown in Fig. 5. Thus, polymers **9a** and **9d** derived from unfunctionalised anhydrides 5 and 8 displayed almost identical spectra, though the C=O peak of polymer **9d** was broader than that of polymer **9a**. The spectra of polymers **9b** and **9c** derived from α,β -unsaturated anhydrides 6 and 7 both showed an additional C=O peak at 165–170 ppm corresponding to a conjugated carbonyl system. This was further supported by the presence of conjugated alkene signals between 120 and 155 ppm. It is known²² that itaconic and citraconic groups can equilibrate under thermal conditions which accounts for both the complexity of the alkene region of the spectra of polymers **9b** and **9c** and their similarity.

The synthesis of polymers **9a–d** could be modified to produce polymeric disks (*ca.* 3 cm diameter and 3 mm depth) rather than powders. Epoxidised macaw palm oil 2 was chosen

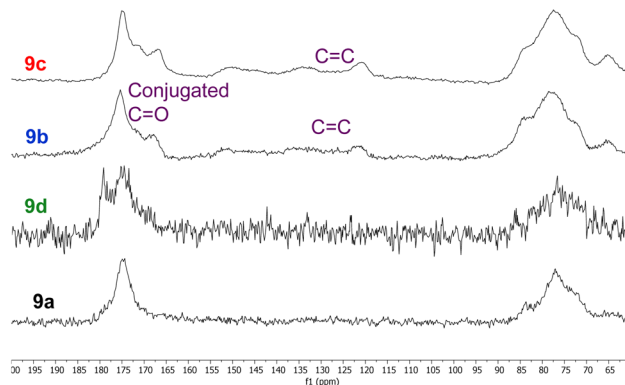


Fig. 5 Comparison of the 60–200 ppm region of the solid-state ^{13}C NMR spectra of polymers **9a–d**.

for this study as it is a liquid at room temperature. Addition of polymerisation initiators 3 and 4 and an anhydride (5–8) followed by warming under nitrogen to 50 °C gave a free flowing homogeneous solution. At this temperature, no polymerisation occurs as shown by DSC analysis of the polymerisation mixture (ESI, Fig. S11[†]). The solution of monomers and initiators could then be poured into an aluminium mould placed within a flat-bottomed flange flask and heated to 100 °C under nitrogen for 18 hours to induce the polymerisation. After cooling to room temperature and removal of the aluminium mould, transparent, yellow–orange disks were obtained as shown in Fig. 6. The Shore A hardness,²³ of the disks were determined using a durometer, giving the results shown in Table 2. All the disks had Shore A hardness values of 60–80 which are comparable to those of car tyre treads (70) and shoe heels (80).²⁰

DSC analysis (–80 to 200 °C) of samples of the polymeric disks identified a glass transition temperature at between –18 and 1 °C for all four polymers as detailed in Table 2 (ESI, Fig. S38–S41[†]). These values are comparable with those obtained for powdered samples of polymers **9a**, **b** and **d**. Polymer **9a** showed a second glass transition at 90 °C. Tan δ values obtained by differential mechanical analysis (DMA) are equivalent to T_g temperatures obtained by DSC. All the disks exhibited tan

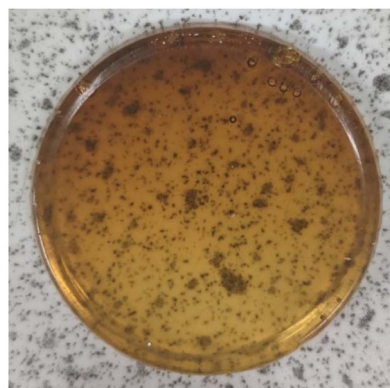


Fig. 6 Polymeric disk obtained from triglyceride 2, anhydride 5 and initiators 3 and 4 (250 : 1000 : 1 : 1 ratio).



Table 2 Physical properties of the polymeric disks

Polymer	Shore A hardness	T_g^a (°C)	$\tan \delta^b$ (°C)	ν^b (mol m ⁻³)	Stress (mPa)	Strain (%)
9a	63	-4.6 (89.9)	0.5	794.8	0.4	11.6
9b	70	-12.6	0.5	408.7	0.4	18.4
9c	72	0.6	17.5	1738.1	0.8	11.3
9d	80	-17.5	-9.4	699.0	0.0005	7.6

^a Glass transition temperature determined by DSC. ^b Determined by DMA.

δ temperatures below room temperature indicating that they are in a rubbery state at 25 °C (ESI, Fig. S42†). These results are consistent with the Shore A hardness values, indicating that the disks are soft and have low rigidity. Below the $\tan \delta$ temperature, the polymers are in the glassy region, turning into a brittle and rigid material. Polymer **9c** has the highest temperature of $\tan \delta$, which can be related to a higher cross-linking density (ν , 1738.1 mol m⁻³).

Tensile strength analysis (ESI, Fig. S43†) indicates that all the polymer disks support stresses below 1 MPa, which can be related to their rubbery state. Furthermore, the strain for each sample did not surpass 20%, as expected for non-linear and cross-linked polymers.^{24,25}

Finally, the ability to chemically degrade the polymers at the end of their life to prevent them accumulating in the environment was investigated. Samples of polymers **9a–d** were exposed to 1 M aqueous sodium hydroxide. Polymers **9a**, **b**, **d** completely dissolved in less than 8 hours whilst polymer **9c** required 24 hours to give a homogeneous solution (ESI, Fig. S44†).

Experimental

Materials and methods

Epoxidized baru nut and macaw palm oils were obtained as previously reported.¹² Other chemicals were obtained from Merck, Sigma-Aldrich or Alfa Aesar and used as received.

Infrared spectra were recorded on a PerkinElmer Spectrum 400 FTIR spectrometer. Solution-state ¹³C NMR spectra were recorded at 100 MHz on a JEOL ECS400 spectrometer and solid-state ¹³C NMR spectra were recorded at 100 MHz on a Bruker AVIII HD 400 WB spectrometer.

DSC traces on powdered samples were acquired using a TA Instruments Q2000 modulated Differential Scanning Calorimeter. DSC curves for disk samples were obtained using a DSC-Q10 modulus controlled by a Thermal Advantage® for Q-Series software v.5.5.24 (both from TA Instruments) using 11.0 ± 0.2 mg of sample, analysed in a 40 µL closed aluminium crucible with a 0.7 mm pin hole in the centre of the lid in cooling/heating stages (-80 to 200 °C) with a dynamic N₂ atmosphere (50.0 mL min⁻¹) and setting a heating rate of 10.0 °C min⁻¹. Measurements of thermal transitions were taken from the final heat-cool cycle (4th or 5th) in all instances. TGA analyses were acquired using a Stanton Redcroft STA 625 instrument.

DMA analyses were carried out using a Q800 apparatus controlled by a Thermal Advantage® for Q-Series software v.5.5.24 (both from TA instruments). The polymer samples were

cut into strips with *ca.* 20 mm length, 6 mm width and 2 mm thickness (±0.02 mm) prior to analysis. Samples were analysed from -80 °C to 80 °C under a N₂ atmosphere, using a frequency of 1 Hz and a heating rate of 3 °C min⁻¹. The DMA provided curves which were used to obtain storage modulus (E') and $\tan \delta$ values. The cross-link density (ν) was determined from the equation ($\nu = E'/3RT$) where E' is the rubbery region storage modulus, R is the gas constant (8.314 J K⁻¹ mol⁻¹), and T (K) is the rubbery temperature ($T_g + 40$ °C). The tensile strength test (stress-strain curves) for each polymer was determined in the same DMA equipment with similar specimens at 25 °C.

Shore A hardness measurements were made using a Sauter 100-0 HBA Shore A Durometer. The needle of the durometer was pushed into polymer disks (**9a–d**) until the hardness value had peaked. In all cases, the peak Shore A is reported and measurements were taken under ambient conditions.

General procedure for the synthesis of powdered polymers 9a–h

To an oven-dried 15 mL sample vial were added DCHU **3** (2.24 mg, 0.01 mmol, 1 eq.), PPNCI **4** (5.7 mg, 0.01 mmol, 1 eq.), triglyceride **1** or **2** (2.5 mmol, 250 eq.) and anhydride **5–8** (10 mmol, 1000 eq.). The vial was sealed, purged with N₂, then heated to 100 °C for 18 hours. After cooling to room temperature, the polymerisation mixture was ground to a powder and placed in a cellulose Soxhlet extraction thimble. Extraction of initiators and unreacted monomers using CH₂Cl₂ until the polymer reached constant weight left polymers **9a–h** as white–yellow powders. EtOAc or EtOH could also be used as greener extraction solvents and were only marginally less effective than CH₂Cl₂ (4–5%, by weight, less material extracted after 18 hours).

9a. Obtained as a white powder (2.29 g, 2.42 mmol) in 67% yield. ν_{\max} 2926, 2855 and 1733 cm⁻¹; δ_C (100 MHz, solid) 174.9, 77.0, 34.8, 32.3, 27.8, 25.6 and 16.9 ppm; TGA (10% weight loss) 340 °C; DSC (glass transition temperature) -5.0 °C.

9b. Obtained as a yellow powder (2.17 g, 2.29 mmol) in 61% yield. ν_{\max} 3000, 2970, 2926, 2855, 1737 and 1656 cm⁻¹; δ_C (100 MHz, solid) 175.4, 168.0, 151.0, 135.9, 120.8, 78.1, 65.4, 36.7, 34.8, 32.4, 27.9, 25.6, 23.5 and 16.9 ppm; TGA (10% weight loss) 325 °C; DSC (glass transition temperature) -5.4 °C.

9c. Obtained as a yellow powder (2.11 g, 2.23 mmol) in 59% yield. ν_{\max} 2925, 2855, 1733 and 1653 cm⁻¹; δ_C (100 MHz, solid) 174.8, 171.4, 166.8, 150.5, 134.1, 120.7, 77.2, 65.0, 36.1, 34.5, 32.3, 27.9, 25.5, 23.3 and 16.8 ppm; TGA (10% weight loss) 304 °C; DSC (glass transition temperature) none detected.



9d. Obtained as a white powder (1.63 g, 1.72 mmol) in 46% yield. ν_{\max} 2926, 2855 and 1733 cm^{-1} ; δ_{C} (100 MHz, solid) 179.2, 174.8, 76.6, 34.6, 32.1, 27.9, 25.3, 22.8 and 16.6 ppm; TGA (10% weight loss) 341 °C; DSC (glass transition temperature) −14.9 °C.

9e. Obtained as a white powder (1.26 g, 1.35 mmol) in 35% yield. ν_{\max} 2926, 2949, 2926, 2854 and 1738 cm^{-1} ; δ_{C} (100 MHz, solid) 174.9, 91.3, 84.6, 77.6, 75.2, 67.4, 59.0, 34.6, 32.2, 30.5, 27.3, 25.4 and 16.9 ppm; TGA (10% weight loss) 352 °C; DSC (glass transition temperature) none detected.

9f. Obtained as a yellow powder (1.52 g, 1.63 mmol) in 54% yield. ν_{\max} 2976, 2926, 2855, 1737 and 1656 cm^{-1} ; δ_{C} (100 MHz, solid) 174.3, 91.4, 85.0, 77.4, 74.8, 74.1, 67.6, 32.3, 27.7, 25.3 and 16.8 ppm; TGA (10% weight loss) 339 °C; DSC (glass transition temperature) none detected.

9g. Obtained as a yellow powder (1.67 g, 1.79 mmol) in 59% yield. ν_{\max} 2925, 2854, 1734 and 1655 cm^{-1} ; δ_{C} (100 MHz, solid) 175.2, 167.2, 134.5, 91.4, 84.6, 77.6, 75.0, 74.1, 71.9, 67.7, 64.8, 59.7, 36.6, 34.6, 32.1, 27.7, 25.3 and 16.6 ppm; TGA (10% weight loss) 334 °C; DSC (glass transition temperature) none detected.

9h. Obtained as a white powder (1.31 g, 1.40 mmol) in 46% yield. ν_{\max} 2925, 2854 and 1733 cm^{-1} ; δ_{C} (100 MHz, solid) 175.0, 91.4, 84.4, 77.6, 74.8, 74.1, 67.6, 65.0, 60.1, 36.3, 34.6, 32.1, 27.7, 25.3, 23.2, 20.8 and 16.8 ppm; TGA (10% weight loss) 356 °C; DSC (glass transition temperature) −13.6 °C.

General procedure for the synthesis of polymer disks 9a–d

To an oven-dried 15 mL sample vial were added DCHU 3 (2.2 mg, 0.01 mmol, 1 eq.), PPNCl 4 (5.7 mg, 0.01 mmol, 1 eq.) and epoxidised macaw palm oil 2 (2.4 g, 2.5 mmol, 250 eq.). The vial was sealed, purged with N_2 , then warmed to 50 °C for 30 minutes. After this time, anhydride 5–8 (10.0 mmol, 1000 eq.) was added. The vial was resealed, purged with N_2 , then warmed to 50 °C until a homogeneous solution formed (*ca.* 5 minutes). The pre-polymerisation solution was poured into a circular aluminium mould (3 cm diameter) which was placed into a flat-bottomed flange flask. The flask was sealed and flushed with nitrogen, then heated to 100 °C for 18 hours. After cooling to room temperature, the flange flask was opened and the polymer removed from the aluminium mould to give polymers 9a–d as yellow–orange disks.

9a. Combustion analysis, found: C, 65.2; H, 8.7; N, 0.2%; Shore A hardness 63; DSC (glass transition temperature) −4.4 and 89.9 °C; DMA $\tan \delta$ 0.4 °C, stress 0.4 MPa, strain 11.6%, cross-linking density 794.8 mol m^{-3} .

9b. Combustion analysis, found: C, 65.5; H, 8.9; N, 0.2%; Shore A hardness 70; DSC (glass transition temperature) −12.7 °C; DMA $\tan \delta$ 0.5 °C, stress 0.4 MPa, strain 18.4%, cross-linking density 408.7 mol m^{-3} .

9c. Combustion analysis, found: C, 65.9; H, 8.7; N, 0.2%; Shore A hardness 72; DSC (glass transition temperature) 0.9 °C; DMA $\tan \delta$ 17.5 °C, stress 0.8 MPa, strain 11.3%, cross-linking density 1738.1 mol m^{-3} .

9d. Combustion analysis, found: C, 66.1; H, 8.8; N, 0.2%; Shore A hardness 80; DSC (glass transition temperature) −17.4 °C; DMA $\tan \delta$ −9.4 °C, stress 0.0005 MPa, strain 7.6%, cross-linking density 699.0 mol m^{-3} .

Conclusions

Ring-opening copolymerisation of epoxidised Brazilian triglycerides and biomass derivable anhydrides can be used to produce bio-derivable, highly crosslinked polyesters. The polymerisation is induced by non-metallic initiators and requires no special precautions (glove box *etc.*) to avoid chain-transfer due to adventitious water. The polymers can be produced as either powders or disks and their spectral and physical properties are dominated by those of the triglyceride from which they were prepared. The polymers were totally degraded to soluble components in 8–24 hours on treatment with 1 M aqueous sodium hydroxide. Thus, the polymers are both sustainably sourced and at end of life can be treated to prevent their accumulation in the environment.

Author contributions

Aaron L. Vermiglio: investigation. Rafael T. Alarcon: investigation, resources, writing – original draft. Éder T. G. Cavalheiro: data curation, funding acquisition, writing – review and editing. Gilbert Bannach: supervision, funding acquisition, project administration, writing – review and editing. Thomas J. Farmer: supervision, writing – original draft. Michael North: conceptualisation, data curation, supervision, project administration, writing – original draft.

Conflicts of interest

There are no conflicts to declare.

Acknowledgements

The authors wish to thank São Paulo Research Foundation – FAPESP (grant 2019/22217-8; 2021/14879-0, and 2021/02152-9) and National Council for Scientific and Technological Development-CNPq (grant 303247/2021-5).

Notes and references

- <https://www.european-bioplastics.org/market/>, accessed 1 November, 2022.
- R. Geyer, J. R. Jambeck and K. L. Law, *Sci. Adv.*, 2017, **3**, e1700782.
- M. Eriksen, L. C. M. Lebreton, H. S. Carson, M. Thiel, C. J. Moore, J. C. Borerro, F. Galgani, P. G. Ryan and J. Reisser, *PLoS One*, 2014, **9**, e111913; E. van Seville, C. Wilcox, L. Lebreton, N. Maximenko, B. D. Hardesty, J. A. van Franeker, M. Eriksen, D. Siegel, F. Galgani and K. L. Law, *Environ. Res. Lett.*, 2015, **10**, 124006; J. R. Jambeck, R. Geyer, C. Wilcox, T. R. Siegler, M. Perryman, A. Andrady, R. Narayan and K. L. Law, *Science*, 2015, **347**, 768–771.
- R. A. Sheldon and M. Norton, *Green Chem.*, 2020, **22**, 6310–6322; J.-P. Lange, *Energy Environ. Sci.*, 2021, **14**, 4358–4376; S. A. Backer and L. Leal, *Acc. Chem. Res.*, 2022, **55**, 2011–2018.



- 5 M. Vert, *Biomacromolecules*, 2005, **6**, 538–546; G. X. De Hoe, T. Şucu and M. P. Shaver, *Acc. Chem. Res.*, 2022, **55**, 1514–1523; R. Yang, G. Xu, B. Dong, X. Guo and Q. Wang, *ACS Sustainable Chem. Eng.*, 2022, **10**, 9860–9871; Y. Liu, Z. Yu, B. Wang, P. Li, J. Zhu and S. Ma, *Green Chem.*, 2022, **24**, 5691–5708.
- 6 J. H. Park, J. Y. Jeon, J. J. Lee, Y. Jang, J. K. Varghese and B. Y. Lee, *Macromolecules*, 2013, **46**, 3301–3308.
- 7 W. A. MacDonald, *Polym. Int.*, 2002, **51**, 923–930.
- 8 X. Zhang, M. Fevre, G. O. Jones and R. M. Waymouth, *Chem. Rev.*, 2018, **118**, 839–885.
- 9 *Ullmann's Encyclopedia of Industrial Chemistry*, Wiley-VCH, Weinheim, vol. A21, pp. 233–238.
- 10 Y. Shen, X. Fu, W. Fu and Z. Li, *Chem. Soc. Rev.*, 2015, **44**, 612–622.
- 11 A. Stopper, T. Rosen, V. Venditto, I. Goldberg and M. Kol, *Chem.–Eur. J.*, 2017, **23**, 11540–11548.
- 12 S. Paul, Y. Zhu, C. Romain, R. Brooks, P. K. Saini and C. K. Williams, *Chem. Commun.*, 2015, **51**, 6459–6479; J. M. Longo, M. J. Sanford and G. W. Coates, *Chem. Rev.*, 2016, **116**, 15167–15197; D. R. G. Printz, B. Jacques, S. Messaoudi, F. Dumas, S. Dagorne and F. Le Bideau, *Polym. Chem.*, 2021, **12**, 2932–2946; X. Liang, F. Tan and Y. Zhu, *Front. Chem.*, 2021, **9**, 647245; A. J. Plajer and C. K. Williams, *Angew. Chem., Int. Ed.*, 2022, **61**, e202104495; W. T. Diment, W. Lindeboom, F. Fiorentini, A. C. Deacy and C. K. Williams, *Acc. Chem. Res.*, 2022, **55**, 1997–2010.
- 13 M. N. D. Haslewood, T. J. Farmer and M. North, *J. Polym. Sci.*, 2023, **61**, 311–322.
- 14 R. T. Alarcon, C. Gaglieri, K. J. Lamb, M. North and G. Bannach, *Ind. Crops Prod.*, 2020, **154**, 112585.
- 15 R. T. Alarcon, K. J. Lamb, G. Bannach and M. North, *ChemSusChem*, 2021, **14**, 169–188.
- 16 L. Lin, J. Liang, Y. Xu, S. Wang, M. Xiao, L. Sun and Y. Meng, *Green Chem.*, 2019, **21**, 2469–2477.
- 17 B. Neises and W. Steglich, *Angew. Chem., Int. Ed. Engl.*, 1978, **17**, 522–524; N. L. Benoiton, *Chemistry of Peptide Synthesis*, CRC Press, Boca Raton, FL, 2016.
- 18 M. Jiang, J. Ma, M. Wu, R. Liu, L. Liang, F. Xin, W. Zhang, H. Jia and W. Dong, *Bioresour. Technol.*, 2017, **245**, 1710–1717.
- 19 M. Zhao, X. Lu, H. Zong, J. Li and B. Zhuge, *Biotechnol. Lett.*, 2018, **40**, 455–464.
- 20 J. H. Crowell, Production of itaconic and citraconic anhydrides, *US Pat.* 2258947, 1941.
- 21 A. Besrat, C. E. Polan and L. M. Henderson, *J. Biol. Chem.*, 1969, **244**, 1461–1467.
- 22 A. Takasu, M. Ito, Y. Inai, T. Hirabayashi and Y. Nishimura, *Polym. J.*, 1999, **31**, 961–969.
- 23 <https://www.smooth-on.com/page/durometer-shore-hardness-scale/>, accessed on 21 November, 2022.
- 24 C. Gaglieri, R. T. Alarcon, R. Magri, M. North and G. Bannach, *J. Appl. Polym. Sci.*, 2021, **139**, e52990.
- 25 C. Di Mauro, S. Malburet, A. Genua, A. Graillot and A. Mija, *Biomacromolecules*, 2020, **21**, 3923–3935.

